

PENETRATION OF CONFINED ALUMINUM NITRIDE TARGETS BY TUNGSTEN LONG RODS AT 1.5–4.5 km/s

D. L. ORPHAL[†], R. R. FRANZEN[†], A. J. PIEKUTOWSKI[‡] and
M. J. FORRESTAL^{*}

[†]Titan Corporation, 5117 Johnson Drive, Pleasanton, CA 94578-3343, U.S.A., [‡]University of Dayton Research Institute, Dayton, OH 45469-0182, U.S.A. and ^{*}Sandia National Laboratories, Albuquerque, NM 87185-0312, U.S.A.

(Received 31 May 1995; in revised form 25 August 1995)

Summary—A series of 26 terminal ballistics experiments was performed to measure the penetration of simple confined aluminum nitride targets by a long tungsten rod. Impact velocities ranged from 1.5 to about 4.5 km/s. The experiments were performed in the reverse ballistic mode using a two-stage light-gas gun. Penetrator diameter, D , was 0.762 mm (0.030 in). The length-to-diameter ratio for the penetrator was $L/D = 20$ for nearly all the tests and never less than $L/D = 15$. Primary instrumentation for these experiments was four independently timed, 450 kV flash X-rays. These X-rays provided four views of the penetrator–target interaction during the penetration event from which the following data were determined: p = penetration depth as a function of time, L_r = remaining length of penetrator as a function of time, as well as final penetration depth, target hole geometry, spatial distribution of the eroded rod material, etc. From these data, $u = dp/dt$ = speed of penetration into the target and $v_c = d(L - L_r)/dt$ = speed of “consumption” of the long rod were obtained.

Key words: hypervelocity, long rods, penetration, ceramics, aluminum nitride, impact, scaling, mass efficiency, armor, Tate model.

INTRODUCTION AND BACKGROUND

Until very recently, armor has been made almost exclusively of metals of one type or another and in various geometries. Depth of penetration of long rod penetrators of various materials against armor steels and aluminum as a function of impact velocity has been established for some time (e.g. Hohler and Stilp [1, 2]; Sorensen *et al.* [3]).

Recently, new materials have been introduced into both light and heavy armors to improve resistance to penetration and reduce weight. One class of such new materials is ceramics. This paper reports experimental data for penetration of a confined aluminum nitride (AlN) ceramic by long tungsten rods at impact velocities from 1.5 km/s to about 4.5 km/s.

EXPERIMENT DESIGN

In order to achieve the large range of impact velocities of interest, the experiments were performed using a two-stage light-gas gun with a 115 mm diameter pump tube and a 38 mm diameter launch tube or barrel. The experiments were performed in the reverse ballistic mode with the confined ceramic target launched at the desired velocity and impacted against a stationary tungsten long rod penetrator. The reverse ballistic test mode was selected because of two very important advantages. First, the targets are sufficiently small that multiple flash X-rays can be obtained of the penetrator inside the target during the penetration process. Thus the dynamics of the penetration process can be investigated as opposed to only measuring the final depth and geometry of the target hole after the test. Second, one has very precise control over such important variables as angle of attack. In all these tests the angle of attack was zero.

The disadvantage of using the reverse ballistic mode is that, with available two-stage light-gas guns, the target, and thus the experiment, must be small scale. While the question of scaling has been investigated often for metal targets, scaling data are much more limited for the case of confined ceramic targets. Data for semi-infinite metal targets generally scale, particularly at higher velocities when the penetration mechanics approaches that

for hydrodynamic materials. The issue of scaling for the data reported here is addressed below.

Primary instrumentation for these experiments was four independently timed, 450 kV flash X-rays. These X-rays provided four views of the penetrator-target interaction during the penetration event. In addition, two continuous X-rays were positioned uprange of the impact. The motion of the target sequentially interrupted the continuous X-rays, giving a transit time over a fixed 0.300 m distance and thus the velocity of the target or the impact velocity. The four 450 kV flash X-rays were also used as an independent check on the impact velocity and to establish an absolute zero time of impact. Target velocity determined by the two independent sets of data were always in excellent agreement.

The performance of an armor can depend greatly on the specifics of the combinations of materials and geometries used. The objective of this research was simply to measure and understand the response of just the ceramic to impact and penetration. Ideally, the targets for this research would be simply cylinders of AlN with a length such that the target would effectively be semi-infinite in depth, and with a diameter sufficiently large that no lateral boundaries are involved during the time of the experiment. This ideal could not, of course, be completely achieved but was, we believe, sufficiently approximated to satisfy the objective of this research.

Figure 1 shows the two target designs used for these experiments. The principal difference between the two targets is the total length. At the lower range of impact velocities of interest

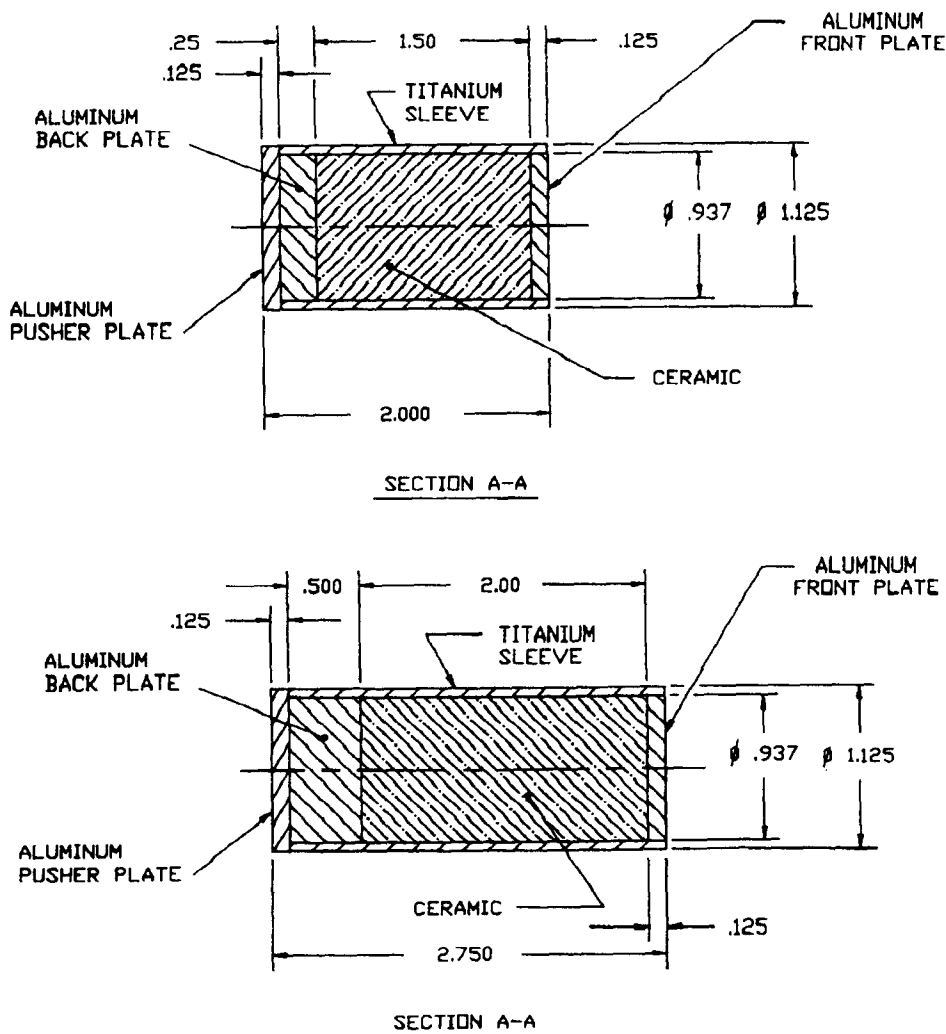


Fig. 1. Confined AlN targets used for reverse ballistic experiments (dimensions in inches).

($1.5 < v \leq 3.7$ km/s) the longer target was used. For velocities $3.7 \leq v \leq 4.5$ km/s, the shorter target was generally used. The targets were designed so that the tungsten penetrator was completely eroded and the final hole in the target formed well within the ceramic. Except for the elastic wave, the aluminum (6061-T6) back plate is not believed to be involved in the penetration process. The aluminum back plate was used primarily to aid in maintaining the integrity of the ceramic cylinder during launch.

All targets also had an aluminum (6061-T6) "cover plate". A cover plate was used because there are some data that suggest that the ballistic performance of some ceramics is improved by inclusion of a cover plate. Also an aluminum cover plate aided in maintaining integrity of the target during launch.

Ideally, the target diameter should be sufficiently large such that no elastic wave could propagate to the radial boundary and back to the axis of symmetry of the target during the penetration event. In this case, the ceramic would be "self-confined". The constraints of the available gun precluded such an ideal approach. The design approach selected was to make the diameter of the ceramic as large as possible. The diameter of the ceramic was 23.8 mm (0.937 in.). Thus, the ratio of the ceramic diameter to penetrator diameter was about 31. In addition, a 2.39 mm (0.094 in.) thick titanium sleeve was placed around the ceramic cylinder to further enhance radial confinement. Finally, around the target shown in Fig. 1 was a cylindrical lexan sabot with an outer diameter of 38 mm (1.5 in.), the diameter of the launch tube. Examination of the flash X-rays from these experiments reveals no significant radial expansion of the targets. Therefore, it is believed that these targets represent what is often described as "well confined" targets.

The AlN used in these experiments was hot-pressed by the Dow Chemical Company. Typical grain size was 1.5 micron. The density was 3.25 g/cm^3 . Additional information on the AlN is given by Orphal and Franzen [4].

The long-rod penetrators were right circular cylinders of pure (99.95%) tungsten ($\rho_p = 19.3 \text{ g/cm}^3$). The penetrator diameter was $D = 0.762 \text{ mm}$ (0.030 in.). For tests using the target with the 2 in. long AlN cylinders, the penetrator L/D was 20. For the highest velocity tests (> 3.7 km/s) using the shorter target, penetrator L/D was reduced to 15 to insure that the penetration was fully contained within the target. The tungsten penetrator was stationary in the ballistic range and was suspended on a strip of Scotch tape. The tape was suspended by monofilament nylon threads in an apparatus that allows adjustment of the penetrator to insure a zero angle of attack, a procedure used successfully on numerous past experiments (e.g. Orphal and Franzen [5]).

ANALYSIS OF FLASH X-RAYS

The primary data from each experiment are four flash X-rays showing the tungsten rod in the process of penetrating the confined AlN target. A typical set of these flash X-rays is shown in Fig. 2 for Test 273 with an impact velocity of 2.979 km/s. In many of these processed images the aluminum cover plate is not readily visible[†]. In these tests the X-ray magnification factor is about 1.15.

The time between each X-ray is known to within less than a 1 μs . Prior to each test four tare X-rays are taken from four different angles showing the position of the tungsten rod relative to fixed spatial fiducials. Since each X-ray shows both the target and a fixed spatial fiducial, the velocity of the target and time of impact can be calculated. Then the known time intervals between X-rays are used to calculate time from impact or "absolute time" for each X-ray. The target velocity is also independently measured using the uprange continuous X-ray system. The velocities determined independently by these two methods have always been in excellent agreement, typically within about 1%.

[†] In these X-rays the dark "ring" at the front of the target is associated with the sabot and is not to be confused with the aluminum cover plate. The fixed spatial fiducials for the X-rays in Fig. 2 are not always visible because the field of view of this computer enhanced X-ray was limited; all fiducials are of course visible in the original X-rays.

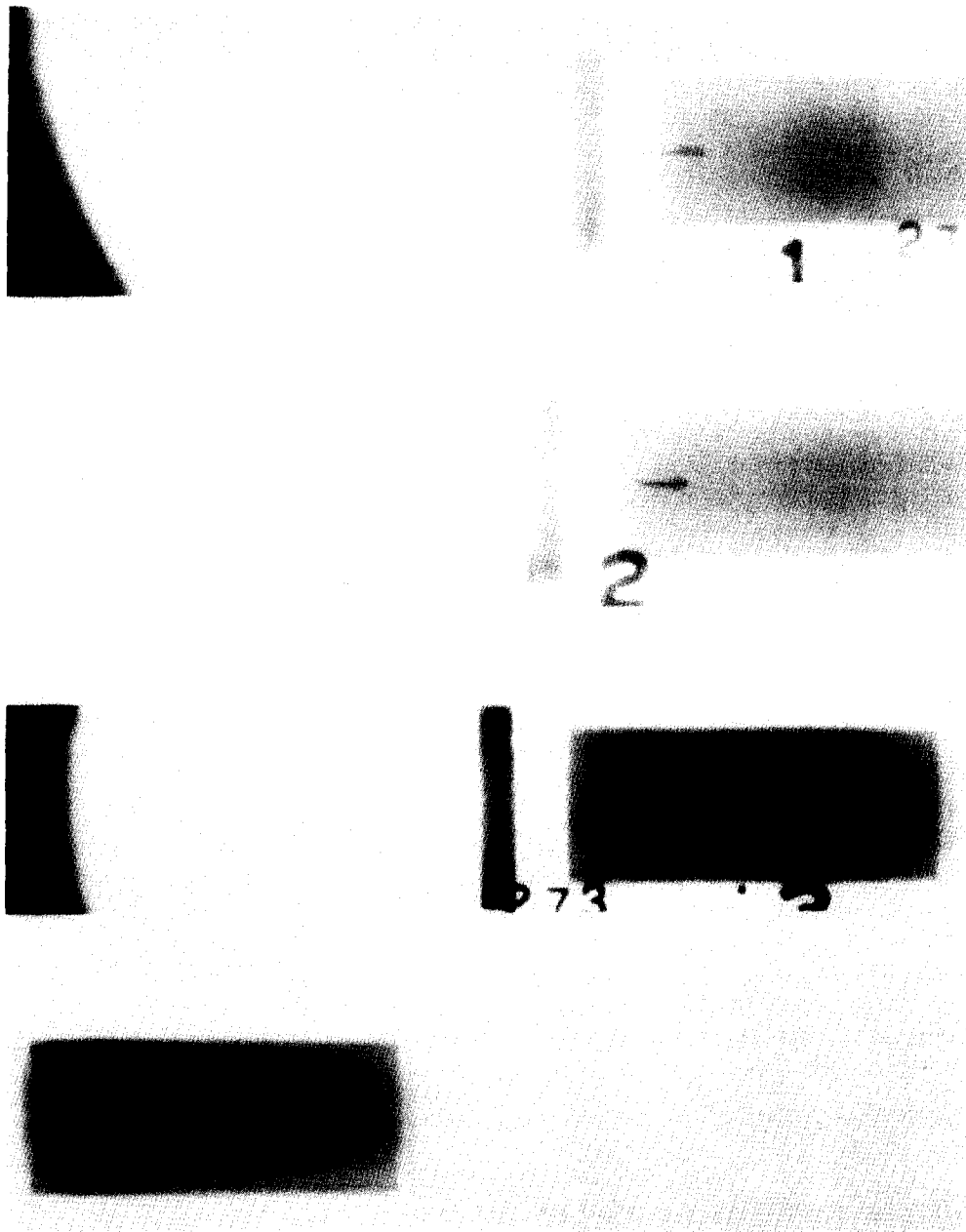


Fig. 2. Flash X-rays from Test 273 showing long tungsten rod penetrating confined AlN target at four different times.

The depth of penetration is measured in each X-ray. (In these tests, no correction was made for the thickness of the aluminum cover plate.) The length of tungsten rod remaining, L_r , is also measured in each X-ray. The measured L_r subtracted from the known initial length of the rod, L , gives the length of rod consumed, $L_c = L - L_r = \text{consumed length}$.

Measured depths of penetration and consumed penetrator length are tabulated for each test. Tabulated data for Test 273 are shown in Fig. 3 along with plots of penetration depth, and consumed rod length vs time from impact. These data include the (0, 0) point since time of impact is independently measured.

Before proceeding, it will be useful to define several important parameters:

Penetration velocity, u . As can be seen from Fig. 3, the first four points of the penetration vs time plot, including (0, 0), are fitted well by a straight line of slope $dp/dt = u = 1.876 \text{ km/s}$ (correlation coefficient = 0.999). This slope is defined as the penetration velocity.

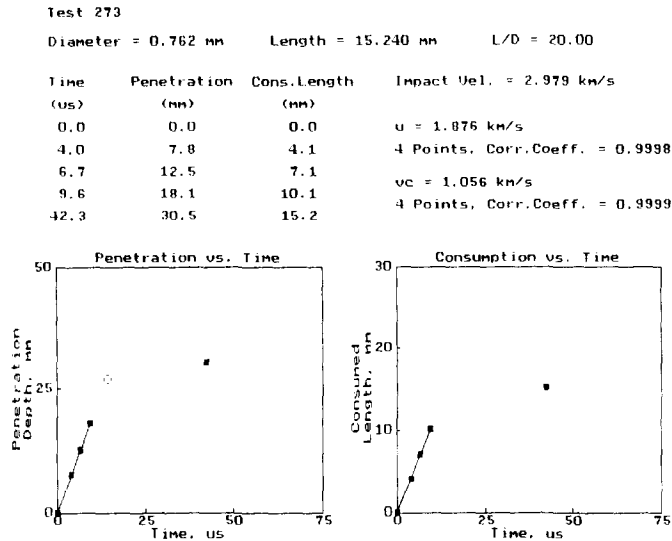


Fig. 3. Summary of typical test data.

Consumption velocity, v_c . The first four points of the consumed penetrator length vs time plot in Fig. 3, including (0,0), are fitted well by a straight line of slope $dL_c/dt = 1.056 \text{ km/s} = v_c$ (correlation coefficient = 0.999). This slope is defined as the consumption velocity, v_c .

Primary penetration depth. To a good first approximation, it may be assumed for these high L/D tungsten rods that the rear of the rod does not decelerate until it reaches the rod/target interface*. With this approximation, the time required for the rear of the rod to reach the rod/target interface is simply $t_c = L/v_c$. The depth of penetration at the time t_c is defined here as the primary penetration, $p_{\text{primary}} = ut_c = u(L/v_c)$. In Fig. 3, p_{primary} is shown as the open symbol on the penetration depth vs time plot.

Total penetration depth. For each test one of the flash X-rays was timed to fire long after the tungsten rod had been completely eroded or consumed (but before the target had traveled beyond the field of view of the X-rays). The depth of penetration measured in this "late-time" X-rays is defined as the total penetration depth, p_{total} .

PHENOMENOLOGY

Phenomenology observed for long rod penetration of confined 'AlN' differs in some interesting ways from observations for metal targets under the same conditions. This discussion attempts to highlight briefly some of these differences; more detail can be found in Orphal and Franzen [4].

For an impact velocity of 1.5 km/s the penetration of the long tungsten rod into AlN appears essentially steady-state throughout the penetration event, i.e. $u = \text{constant}$ (Orphal and Franzen [4]). At this impact velocity the geometry of the rod/target interaction region ("mushroom") is very irregular and asymmetric, as is the geometry of the rod debris behind the penetration front. If the geometry of the eroded rod debris in any way corresponds to the inner surface of the hole in the target, this hole geometry may also be highly irregular. At 1.5 km/s there is a significant accumulation of debris from the tungsten rod between the aluminum cover plate and the ceramic. Also, even in the last X-ray, long after the rod is completely eroded, tungsten debris can be seen distributed along the penetration hole essentially all the way to the cover plate. This seems to imply that the tungsten debris has

*This is not strictly true, especially for the lower velocity tests.

a very low velocity relative to the target. Some of these phenomena seem very similar to phenomena observed by Hauver (personal communication) in his reverse ballistic experiments at a similar scale and his direct ballistic experiments at a much larger scale at about 1.5 km/s.

At the slightly higher impact velocity of 1.653 km/s the penetration appears to be essentially steady state throughout all the primary penetration phase. The rod/target interface geometry is still irregular, as is the distribution of rod debris along the penetration path, generally very similar to the 1.5 km/s impact. Again, even at late time, rod debris is observed essentially all the way to the cover plate. Some tungsten debris accumulates along the interface between the ceramic and cover plate but the radial extent of this accumulation is significantly less than observed at 1.5 km/s.

At an impact velocity of about 2 km/s the penetration is steady state and the rod/target interface symmetry is much more regular. Tungsten debris behind the penetration front is fairly regular and, again, even at late times extends all the way to the cover plate. At this impact velocity there is very little noticeable accumulation of tungsten debris at the interface between the cover plate and ceramic. There is little or no noticeable debris accumulation at this interface in any test with an impact velocity of 2 km/s or higher. As impact velocity increases beyond 2 km/s the rod/target interface geometry becomes increasingly symmetric and the tungsten rod debris more regular. Even at the highest velocities, tungsten rod debris is observed to extend essentially all the way to the cover plate at late times.

PENETRATION VS IMPACT VELOCITY DATA

In discussing the penetration data for confined AlN, comparisons will sometimes be made with “ideal hydrodynamic theory” (Birkhoff *et al.* [6]). For ideal hydrodynamic behavior,

$$u = v \left/ \left(1 + \sqrt{\frac{\rho_t}{\rho_p}} \right) \right. \quad \text{and} \quad p = L \sqrt{\frac{\rho_p}{\rho_t}}. \quad (1) \quad (2)$$

Penetration velocity, u

For these experiments the penetration is observed to be steady-state (i.e. $u = dp/dt = \text{constant}$) to a high degree of approximation over the entire impact velocity range from 1.5 to 4.5 km/s. Figure 4 shows penetration velocity impact velocity for each of these confined AlN tests, along with the ideal hydrodynamic penetration velocity. Measured penetration velocities are less than expected from hydrodynamic theory over the entire 1.5–4.5 km/s range of impact velocities tested. The penetration velocity data are fitted quite well with the simple linear equation $u = 0.792v - 0.524$ (km/s).

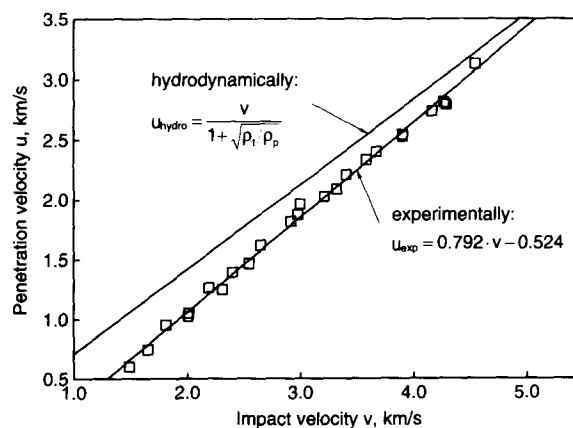


Fig. 4. Penetration velocity as a function of impact velocity for long tungsten rods impacting confined AlN targets.

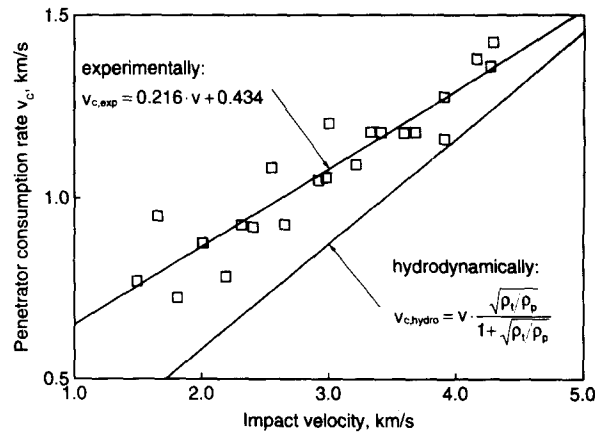


Fig. 5. Penetrator consumption rate as a function of impact velocity for long tungsten rods impacting confined AlN targets.

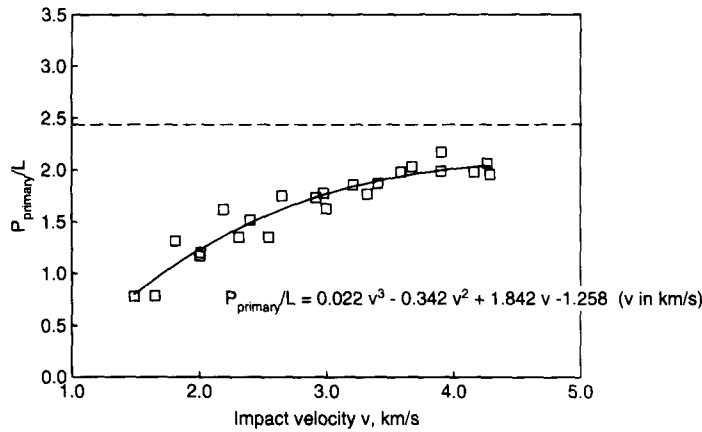


Fig. 6. Primary penetration depth as a function of impact velocity for long tungsten rods impacting confined AlN targets.

Consumption velocity, v_c

Figure 5 shows the data for v_c vs impact velocity along with the ideal hydrodynamic consumption velocity, $(v - u)$, where u is calculated from hydrodynamic theory. The measured consumption velocity for confined AlN exceeds the ideal hydrodynamic value over the entire 1.5–4.5 km/s range of impact velocity tested. Although there is significant scatter, the v_c data can reasonably be represented by the simple linear equation $v_c = 0.216v + 0.434$ (km/s).

Primary penetration, p_{primary}

Figure 6 shows primary penetration normalized by the original projectile length, L , as a function of velocity. Also shown is the ideal hydrodynamic value for p/L of 2.44 (dashed line). The measured primary penetration is less than the ideal hydrodynamic value over the entire 1.5–4.5 km/s range of impact velocity tested. There is significant scatter in the data, seemingly greater than typically measured for total penetration in metal targets (e.g. Hohler and Stilp [1, 2]).

The measured (p_{primary}/L) data have been least-squares fitted using a cubic equation which gives $p_{\text{primary}}/L = (-1.258) + 1.842v - 0.342v^2 + 0.022v^3$ (km/s). The resulting curve is shown in Fig. 6. A number of mathematical forms have been tried to fit this penetration vs impact velocity data. The most successful form so far is the cubic equation (for example the hyperbolic equation developed by Sorensen *et al.* [3] and reported in Anderson and Morris [7] fails). A cubic fit does not asymptote to a “hydrodynamic limit” as $v \rightarrow \infty$ (and neither

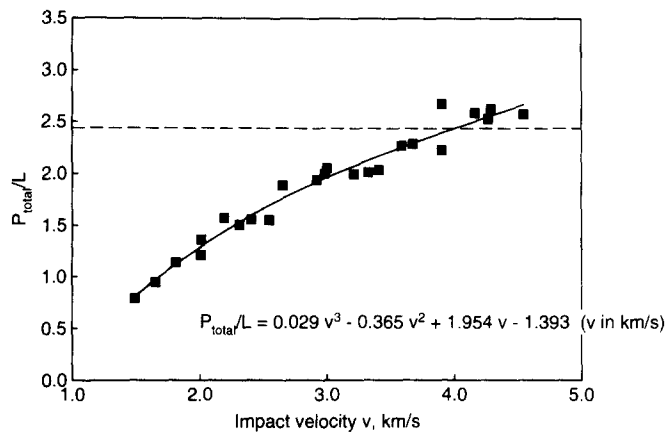


Fig. 7. Total penetration depth as a function of impact velocity for long tungsten rods impacting confined AlN targets.

does the hyperbolic developed by Sorensen *et al.*). The cubic fit does however represent the data well and is mathematically convenient. This cubic fit is purely empirical, of course, and should not be used outside the range of the data.

Total penetration, p_{total}

Figure 7 shows the total penetration data vs impact velocity along with the value for the ideal hydrodynamic penetration (dashed line). It is only for impact velocities of about 4 km/s and higher that the measured total penetration essentially equals the hydrodynamic value[†]. A cubic equation was used to least-squares fit the (p_{total}/L) data giving $p_{\text{total}}/L = (-1.393) + 1.954v - 0.365v^2 + 0.029v^3$ (km/s). The resulting cubic fit is shown in Fig. 7. Again, this cubic equation is purely empirical and should not be used outside the range of the data.

Strictly speaking ideal hydrodynamic theory applies to what is called here the primary penetration. It therefore is of interest that the hydrodynamic limit for AlN is not achieved for p_{primary} even at an impact velocity as high as 4.5 km/s. At an impact velocity of 4.5 km/s (p_{primary}/L) for these confined AlN targets is only about 85% of the hydrodynamic limit.

Even for (p_{total}/L) , which now includes residual penetration (Hohler and Stilp [2]), the hydrodynamic limit is only achieved for impact velocities greater than about 4 km/s. This is to be contrasted with results for RHA which show that (p_{total}/L) essentially achieves the hydrodynamic limit at impact velocities of 2.5–3 km/s and is 80% of the hydrodynamic limit at an impact velocity as low as 2 km/s.

Examination of the curves in Figs 6 and 7 shows that for impact velocities greater than 2.5–3 km/s, (p_{total}/L) is significantly greater than (p_{primary}/L) . This is a result of residual penetration. Residual penetration for AlN as well as other ceramics is being further studied at this time and the results will be given in a future paper.

SCALING

The experiments described above were performed in the reverse ballistic mode at small scale. The question thus arises regarding the scalability of these experimental results. This is a very complex question which currently is probably best resolved experimentally. That may be accomplished by doing the requisite “full-scale” testing if possible and, in any case, testing at much larger scale than these small scale experiments.

Seven larger scale, direct ballistic, experiments were performed against confined AlN targets by Piekutowski and Forrestal [8]. In these seven experiments an $L/D = 10$ tungsten

[†]Or slightly exceeds the hydrodynamic values because of “residual”, or, as it’s sometimes called, “secondary penetration” or “after-flow” (e.g. Hohler and Stilp [2]).

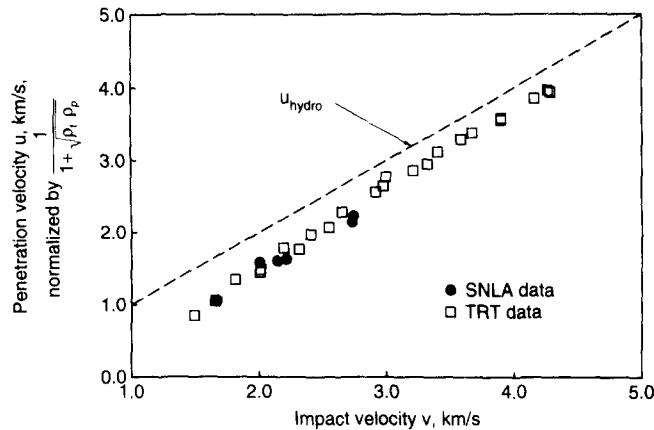


Fig. 8. Comparison of normalized penetration velocities measured in these small-scale reverse ballistic experiments (TRT data) and similar direct ballistic experiments at about six times larger scale (SNLA data).

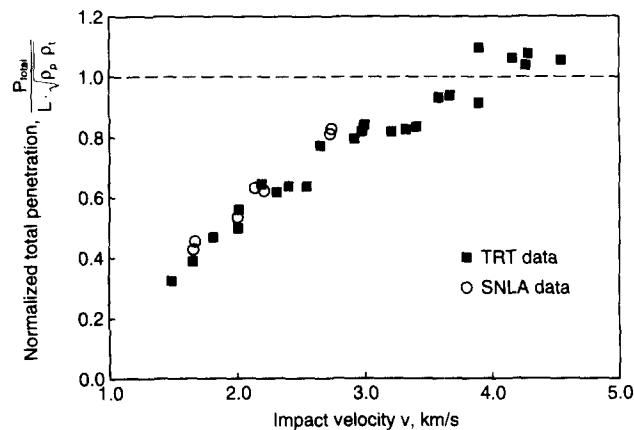


Fig. 9. Comparison of normalized total penetration depth measured in these small-scale reverse ballistic experiments (TRT data) and similar direct ballistic experiments at about six times larger scale (SNLA data).

alloy rod was impacted against a confined AlN target at 1.7, 2.2 and 2.7 km/s. The penetrator was an X21-C ($\rho = 17.65 \text{ g/cm}^3$) rod with 4.57 mm diameter. The rod had a spherical nose and an overall length, including the nose, of 48.0 mm. The diameter of the confined AlN cylinder was 98 mm or about 21 penetrator diameters. Two flash X-rays were used to obtain penetration vs time data. These data were used to calculate penetration velocity. Total penetration depth was measured post-test.

Figure 8 compares the penetration velocity (closed symbols) data measured in these larger scale experiments with those reported here from the small scale reverse ballistic experiments. Similarly Fig. 9 compares the data for total penetration depth from these seven large scale experiments (open symbols) with the data from the small scale reverse ballistic experiments. For penetration velocity and total penetration depth the agreement between these two sets of data is considered very good. The two sets of experiments differ in scale by about a factor of six.

It must be emphasized that the comparisons shown in Figs 8 and 9 do not resolve the question of scaling for these experiments. The data are too few and even the larger scale experiments are only about 1/6 of "full scale". While the comparisons are considered encouraging, questions of scaling will continue to be troublesome until facilities are available to launch full-scale, or at least large-scale, projectiles at real, complex targets at velocities up to 5 km/s and certainly higher than about 2.5 km/s.

ADDITIONAL ANALYSES AND CONSIDERATIONS

The Tate equation: the term $(R_t - Y_p)$

If one assumes for normal impact, that the penetration of a target by a long rod is steady state, and that both the rod and target behave hydrodynamically (i.e. as fluids with no strength) then Bernoulli's equation, $1/2 \rho_p (v - u)^2 = 1/2 \rho_t u^2$ gives the pressure at the rod/target interface on the axis of symmetry. However, materials of interest in ballistics have strength and, particularly at velocities of only 1–2 km/s, these strengths are not necessarily small compared to the terms $1/2 \rho_p (v - u)^2$ and $1/2 \rho_t u^2$. Therefore, Tate [9] and also Alekseevski [10] suggested modifying Bernoulli's equation by adding terms to represent the "strengths" of both the projectile, Y_p , and the target, R_t . Then the pressure at the stagnation point is written $1/2 \rho_p (v - u)^2 + Y_p = 1/2 \rho_t u^2 + R_t$. This modified Bernoulli equation is often called the "Tate equation".

As Tate points out, it is particularly important that the term R_t not be interpreted simply as the shear strength or yield strength of the target material. Bernoulli's equation is one-dimensional and, strictly speaking, it applies only at a single point. The Tate equation of course is a simple scalar modification of Bernoulli's equation. Yet, the penetration of a long rod into a target is a two-dimensional process, assuming axial symmetry. Thus the simple scalar term R_t is an attempt to lump both the strength of the target and these two-dimensional effects into a single parameter. The term R_t is thus perhaps best viewed as a measure of the "overall resistance of the target to penetration".

Regardless of its obvious limitations, the Tate equation has proved very useful in analyzing terminal ballistic data. Thus it is of interest to apply the Tate equation to the data reported here to gain some insight into the magnitude and behavior of the term R_t for these confined AlN targets.

The term $(v - u)$ is the ideal consumption velocity, the difference between the velocity at which rod material flows into the stagnation point, v , and the velocity that the rod/target interface or stagnation point penetrates the target, u . In the experiments reported here the consumption velocity, v_c , was measured independently of u or v , so we rewrite the Tate equation as $R_t - Y_p = 1/2 \rho_t v_c^2 - 1/2 \rho_t u^2$. Figure 10 shows $(R_t - Y_p)$ vs velocity for confined AlN calculated using our data for u and v_c . Also shown as the solid curve is $(R_t - Y_p)$ computed using the least squares fits for u and v_c given above. The curve is *not* a least squares fit to $(R_t - Y_p)$ vs v .

There is a great deal of scatter in the values calculated for $(R_t - Y_p)$. Thus it will only be noted at this time that the general magnitude for the quantity $(R_t - Y_p)$ seems to be in the range of 30–70 kb for these confined AlN targets. If one takes $Y_p = 20$ kb, this implies that $R_t \sim 50$ to 90 kb for confined AlN.

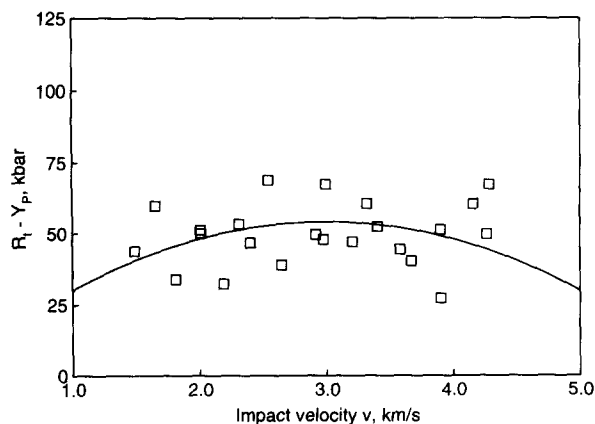


Fig. 10. The Tate term $(R_t - Y_p)$ as a function of impact velocity for long tungsten rods impacting confined AlN targets.

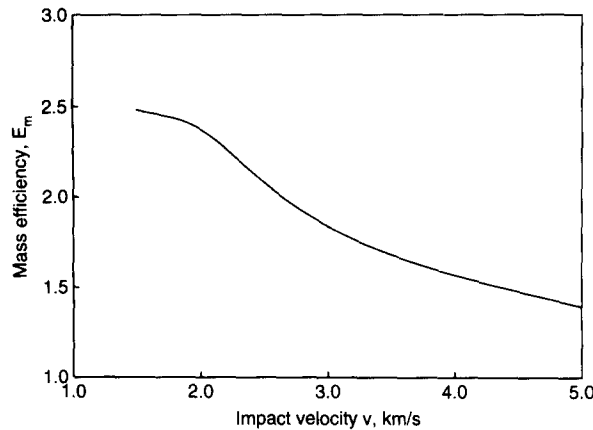


Fig. 11. Mass efficiency, E_m , as a function of impact velocity for long tungsten rods impacting confined AlN targets.

Mass efficiency, E_m

A measure of interest with respect to ceramic armors is the mass efficiency, E_m . E_m is the ratio of the mass per unit area of a steel (RHA) target required to defeat a specified projectile at a specified impact velocity to the mass of a ceramic target required to defeat the same projectile. For semi-infinite targets

$$E_m = \frac{p_{\text{RHA}} \rho_{\text{RHA}}}{p_c \rho_c} \quad (3)$$

where p_{RHA} and p_c are the total penetration depths in the RHA and ceramic target, respectively, and ρ_{RHA} and ρ_c are the densities of RHA and the ceramic.

Figure 11 shows E_m vs impact velocity for these AlN experiments. E_m is greater than one as expected. At 1.5 km/s impact velocity E_m for these AlN targets is about 2.5. E_m is a decreasing function of impact velocity. Again, this is to be expected since (p/L) for these AlN targets approaches the “hydrodynamic limit”, albeit at quite high impact velocity. If both the ceramic and RHA targets were to respond according to ideal hydrodynamic theory then

$$E_m = \sqrt{\rho_{\text{RHA}}/\rho_c}. \quad (4)$$

Penetration for constant projectile L/D and kinetic energy

Any gun system has a maximum energy that can be imparted to any projectile. Furthermore, for a given gun launch cycle, penetrator and sabot materials and design, etc., there is a maximum L/D long rod that can be successfully launched. Thus, a very important question arises regarding the penetration vs velocity curve if both the projectile L/D and kinetic energy are fixed. That is, if one fixes the kinetic energy, then any increase in velocity must result in a decrease in the projectile mass. If the projectile L/D is also fixed, reducing projectile mass requires that both L and D are reduced. Reducing L reduces the penetration depth. The question is whether any gain in penetration depth due to increasing impact velocity exceeds the loss associated with the reduced length of the projectile.

Under the constraints of a cylindrical projectile of constant L/D and kinetic energy, penetration vs velocity can be derived as,

$$p_{\text{total}}/L_0 = \frac{f(v)}{(v/v_0)^{2/3}}$$

where L_0 is the length of the projectile at a reference velocity v_0 and $f(v)$ is the function giving p/L as a function of impact velocity (see total penetration, p_{total}).

Figure 12 is a plot of the p_{total}/L_0 vs impact velocity data for each of these confined AlN reverse ballistic tests under the constraints of constant L/D and kinetic energy, and where

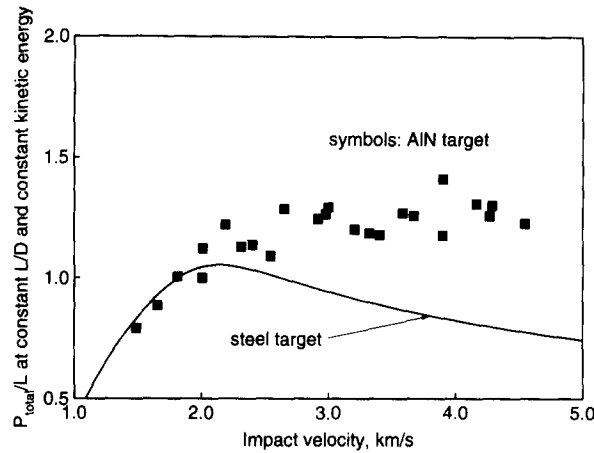


Fig. 12. P_{total}/L at constant penetrator L/D and kinetic energy as a function of impact velocity for long tungsten rods impacting confined AlN and semi-infinite RHA targets.

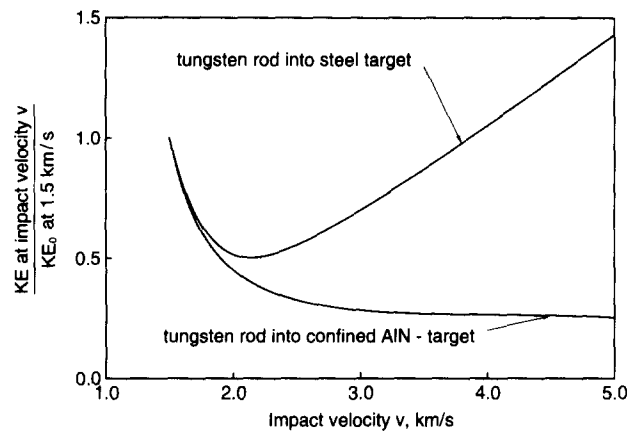


Fig. 13. Relative kinetic energy required for fixed penetration depth as a function of impact velocity for constant L/D long tungsten rods impacting confined AlN and semi-infinite targets.

$v_0 = 1.5$ km/s. Also shown is the curve for RHA using $p/L = f(v)$ developed by Sorensen *et al.* [3] and reported in Anderson and Morris [7]. For confined AlN the maximum occurs at a higher velocity (~ 3 km/s) than for RHA targets (~ 2.2 km/s). Perhaps more importantly, for RHA the curve decreases with increasing impact velocity for $v \geq 2.2$ km/s; while, in contrast, for AlN the curve is more or less constant for $3 \leq v \leq 4.5$ km/s.

Kinetic energy required for fixed penetration depth for constant L/D penetrator

Another comparison of interest is: for a given constant L/D penetrator, what kinetic energy is required to penetrate a specified target? For a semi-infinite target the analogous criterion is the kinetic energy required to penetrate to a fixed depth, p_1 . It is easy to show that, assuming a cylindrical projectile of constant L/D and a constant penetration depth,

$$KE/KE_0 = \left(\frac{v}{v_0} \right)^2 \left[\frac{f(v_0)}{f(v)} \right]^3$$

where KE and KE_0 are the projectile kinetic energies at velocities v and v_0 , respectively. Similarly $f(v)$ and $f(v_0)$ are the functions $p/L = f(v)$, for impact velocities v and v_0 , respectively. This equation was used with the function $p_{\text{total}}/L = f(v)$ given above for AlN to calculate the curve shown in Fig. 13. Also shown in Fig. 13 is the curve for an RHA target

using $P/L = f(v)$ as developed by Sorensen *et al.* [3] and reported in Anderson and Morris [7].

Figure 13 shows the well-known result (which can also be inferred from Fig. 12) that for RHA targets and a constant L/D penetrator the kinetic energy required to penetrate a fixed depth decreases up to a velocity of about 2.2 km/s and then increases for higher impact velocities. For the confined AlN the “minimum” in the curve essentially occurs at around 3 km/s impact velocity and (KE/KE_0) is approximately constant for $3 \leq v \leq 5$ km/s. Also note that for RHA the minimum of (KE/KE_0) is about 0.5. That is for an RHA target, fixing penetrator L/D , only about half the kinetic energy is required to penetrate a given depth at an impact velocity of 2.2 km/s than at 1.5 km/s. The result for confined AlN is even more interesting. For AlN increasing the impact velocity from 1.5 to 3 km/s reduces the total kinetic energy required to achieve a fixed penetration depth by about a factor of four.

CONCLUSIONS

These experiments show that for long tungsten rods impacting simple, confined AlN targets at 1.5–4.5 km/s:

1. target penetration is essentially steady-state over the entire range of impact velocities (i.e. $u = dp/dt = \text{constant}$ for each test),
2. similarly, the consumption rate of the rod is steady-state (i.e. $v_c = d(L - L_r)/dt = \text{constant}$ for each test),
3. primary penetration, $p_{\text{primary}} = L \cdot u/v_c$, is significantly less than ideal hydrodynamic penetration ($= L \cdot \sqrt{\rho_p/\rho_t}$) over the entire impact velocity range 1.5–4.5 km/s,
4. total penetration, which includes residual (or secondary or after-flow) penetration only equals or slightly exceeds ideal hydrodynamic penetration for impact velocities greater than about 4 km/s,
5. the term $(R_t - Y_p)$ from the Tate equation can be determined directly from the experimental data and has a value of about 30–70 kb,
6. the mass efficiency, $E_m = (p_{\text{RHA}} \rho_{\text{RHA}})/(p_c \rho_c)$ for AlN decreases with increasing impact velocity from about 2.5 at 1.5 km/s to about the value expected from ideal hydrodynamic theory of 1.55 at about 4.5 km/s,
8. limited data suggest that the data for penetration velocity and total penetration depth from these small-scale reverse ballistic experiments scale to sizes at least six times larger.

Acknowledgements—The reverse ballistic work was performed under the direction of Col. Tom Kiehne and Dr Peter Kemmey of DARPA and their encouragement and assistance is gratefully acknowledged. Dr Kiehne is now with the Institute for Advanced Technology (IAT) at the University of Texas at Austin. The direct ballistic work was supported by the DoD/DoE Penetration Technology Program.

The reverse ballistic testing for this research was performed by Dr Sue Babcock of Titan. Dick Snedeker of Titan was invaluable in procuring test materials, insuring quality control of the targets, planning the tests and assisting in the analysis of the data. Joan Bentley's assistance in preparing the manuscript is also much appreciated.

REFERENCES

1. V. Hohler and A. J. Stilp, Hypervelocity impact of rod projectiles with L/D from 1 to 32. *Int. J. Impact Engng* **5**, 323–331 (1987).
2. V. Hohler and A. J. Stilp, Long rod penetration mechanics, Chap. 5, in *High Velocity Impact Dynamics* (Edited by Jonas A. Zukas). John Wiley (1990). (Also of interest is Chap. 8, Experimental methods for terminal ballistics and impact physics, by the same authors.)
3. B. R. Sorensen, K. D. Kimsey, G. F. Silsby, D. R. Scheffler, T. M. Sherrick and W. D. de Rosset, High velocity penetration of steel targets. *Int. J. Impact Engng* **11**, 107–119 (1991).
4. D. L. Orphal and R. R. Franzen, Penetration of confined aluminum nitride targets by long tungsten rods at 1.5 to 4.5 km/s. CRT-TR-3294-05, Titan Corporation, Pleasanton, CA (1991).
5. D. L. Orphal and R. R. Franzen, Penetration mechanics and performance of segmented rods against metal targets. *Int. J. Impact Engng* **10**, 427–438 (1990).

6. G. Birkhoff, D. P. McDonald, E. M. Pugh and Sir G. Taylor, Explosives with lined cavities. *J. Appl. Phys.* **19**, 563–582 (1948).
7. C. E. Anderson and B. L. Morris, The ballistic performance of confined Al_2O_3 ceramic tiles. *Int. J. Impact Engng* **12**, 174–187 (1992).
8. A. J. Piekutowski and M. J. Forrestal, Penetration into aluminum nitride targets with $L/D = 10$ tungsten rods at impact velocities of 1.7, 2.2 and 2.7 km/s (U). SAND91-0088.RS9123/90/00007, Sandia National Laboratories, Albuquerque, NM (1991).
9. A. Tate, A theory for the deceleration of long rods after impact. *J. Mech. Phys. Solids* **15**, 387–399 (1967).
10. V. P. Alekseevski, Penetration of a rod into a target at high velocity. *Combustion, Explosion, and Shock Waves* **2**, 63–66 (1966).